AIP | Journal of Applied Physics

Effect of interface state distribution on field effect conductance activation energy in hydrogenated amorphous silicon thin film transistors

ByungSeong Bae and Choochon Lee

Citation: Journal of Applied Physics **68**, 3439 (1990); doi: 10.1063/1.346352
View online: http://dx.doi.org/10.1063/1.346352
View Table of Contents: http://scitation.aip.org/content/aip/journal/jap/68/7?ver=pdfcov
Published by the AIP Publishing

Effect of interface state distribution on field effect conductance activation energy in hydrogenated amorphous silicon thin film transistors

Byung-Seong Bae and Choochon Lee
Department of Physics, Korea Advanced Institute of Science and Technology, P. O. Box 150, Cheongryang, Seoul, Korea

(Received 21 March 1990; accepted for publication 18 May 1990)

The gate voltage dependencies of conductance activation energy of source-drain current are investigated for hydrogenated amorphous silicon thin film transistor. We compared the calculated activation energy with experimental results and discussed the density of gap and interface states in hydrogenated amorphous silicon. The experimental results could be explained by the introduction of the interface state distribution with exponential tails near the conduction band edge in parallel with the bulk gap state distribution.

I. INTRODUCTION

Hydrogenated amorphous silicon (*a*-Si:H) thin film transistors (TFTs) with amorphous silicon nitride (*a*-SiN:H) as gate insulators have been studied extensively by a number of groups owing to their potential applications.

The field effect activation energy $E_a^*(V_g)$ was also measured by several groups.[1–4] The field effect activation energy decreases with the increase of gate voltage, approaching a minimum value of approximately 0.1–0.2 eV. In other words the field effect activation energy remains nearly constant even when the gate voltage is increased further above threshold. The above result is not consistent with the numerical results calculated with the gap density of states of the bulk which are commonly used. To account for the discrepancies, large densities of gap states and interface states of uniform distribution are introduced. But the simple increase in the gap and interface state densities cannot explain the constant field effect activation energy.

In this paper the results of calculation are presented and compared with experiment. And we discuss a model developed to explain the experimental results in view of the distribution of the interface states.

II. CALCULATIONS

Several assumptions are made in this calculation. It is assumed that the material is homogeneous, conduction band edge E_C and Fermi level E_F are independent of temperature, and flat band voltage is constant and zero.

For positive gate voltage the electron accumulation is formed at the interface between the *a*-Si:H and *a*-SiN:H layers and the energy band diagram is shown in Fig. 1. If the surface potential is $V_0(V_g)$ when applied gate voltage is V_g as shown in Fig. 1, then total induced charge per unit area Q_{in} is

$$Q_{in} = -\epsilon_{in}(V_g - V_0)/t_{in}, \qquad (1)$$

where ϵ_{in} is the permittivity of the insulator, t_{in} is the thickness of the insulator. The induced interface charge per unit area Q_{it} is given by

$$Q_{it} = -e\int_{E_V}^{E_C} D(E)[f(E - eV_0) - f(E)]dE, \qquad (2)$$

where e is the electronic charge, $D(E)$ is the interface density of state, and $f(E)$ is the Fermi–Dirac distribution.

With appropriate boundary conditions $V(x)|_{x=t_{si}} = 0$ and $F(x) = dV(x)/dx|_{x=t_{si}} = 0$ the total induced charge density per unit area Q_{is} in the bulk semiconductor is given by[5]

$$Q_{is} = -\left(2\epsilon_{si}\int_0^{V_0}\left|\rho(V')\right|dV'\right)^{1/2}, \qquad (3)$$

where t_{si} is the thickness of the silicon, ϵ_{si} is the permitivity of silicon, $\rho(V')$ is the space charge density when the potential is V'. $\rho(V')$ is given by

$$\rho(V') = -e[n_f(eV') - n_{f0}] - e\int_{E_V}^{E_C} g(E) \times [f(E - eV') - f(E)]dE, \qquad (4)$$

where $g(E)$ is the gap density of states, $n_f(eV')$ is the free-carrier density, and n_{f0} is the thermal equilibrium free-carrier density. Free-carrier density $n_f(eV')$ is approximated as

$$n_f(eV') = N_C \exp[-(E_C - E_F - eV')/kT], \qquad (5)$$

where N_C is the effective density of states and the value of $3\times 10^{16}\ T^{3/2}\ \mathrm{cm}^{-3}$ was used.

Equating the induced charge Q_{in} with $Q_{is} + Q_{it}$,

$$-\epsilon_{in}(V_g - V_0)/\mathrm{tin} = -\left(2\epsilon_{si}\int_0^{V_0}\left|\rho(V')\right|dV'\right)^{1/2} - e\int_{E_V}^{E_C} D(E) \times [f(E - eV_0) - f(E)]dE, \qquad (6)$$

the surface potential V_0 can be determined numerically for given $g(E)$ and $D(E)$.

For given boundary potentials V_0 at $x = 0$ and 0 at $x = t_{si}$, we solved the Poisson equation

$$d^2V(x)/dx^2 = -\rho(x)/\epsilon_{si}. \qquad (7)$$

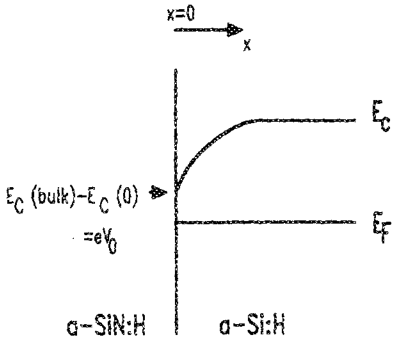

FIG. 1. The band bending at the *a*-SiN:H and *a*-Si:H interface under the positive gate voltage.

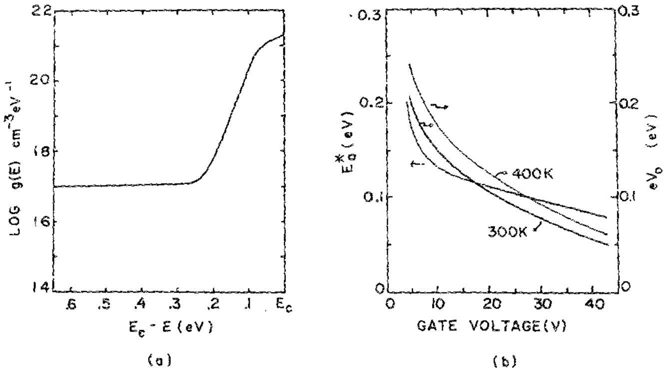

FIG. 2. (a) Model gap density of states of *a*-Si:H. Gap state density of $g(E)$ is an overlap of constant value of 1×10^{17} cm^{-3} eV^{-1} and the band tail having a linear energy dependence down to 0.1 eV from conduction band edge and then decreases exponentially as $\exp[-(E_c-E)/kT_c]$, where characteristic temperature T_c is taken as 200 K. (b) The surface activation energy $E_S=E_c(0)-E_F$ and field effect activation energy E_a^* calculated with the model gap density of states of (a) are plotted against gate voltage. Surface activation energy curves are presented for two different temperatures, 300 and 400 K.

Solving Poisson equation numerically we obtained the potential distribution $V(x)$ over the position x. For the given surface potential V_0, the free-carrier density per unit area $n_s(V_0)$ is

$$n_s(V_0)=\int_0^{t_{si}} n_f[eV(x)]dx. \tag{8}$$

Then, when the source-drain voltage is V_{sd}, the source-drain current is calculated numerically by[6]

$$I_{sd}(V_g)=e\mu_0 W/L\int_{V_g-V_{sd}}^{V_g} n_s[V_0(V)]dV, \tag{9}$$

where μ_0 is the band mobility, W is the channel width, and L is the channel length. These are all assumed constant and independent of temperature and bias. Source drain current I_{sd} was calculated for several temperatures, typically 300, 325, 350, and 400 K. Then, at each gate voltage the field effect activation energy $E_a^*(V_g)$ was obtained from the linear least-square fit of log I_{sd} vs $1/T$.

In this paper the integration from E_V to E_C was approximated by the integration from E_F to E_C. Therefore the band bending upward was not considered and the calculation has the meaning only for the gate voltage larger than the V_{sd}.

III. RESULTS AND DISCUSSIONS

Model gap density of states of *a*-Si:H is shown in Fig. 2 (a). In the region of deep states we assumed a constant density of states since details of shapes of deep states does not have a large effect on above or near threshold gate voltage. Instead our concern is the density of states near the conduction band edge, not near the Fermi level. In Fig. 2(a), gap density of $g(E)$ has a linear energy dependence down to 0.1 eV from conduction band edge, and then decreases exponentially as $\exp[-(E_c-E)/kT_c]$, where T_c is taken as 200 K. The interface density of states is not considered in this case so that interface density of states $D(E)=0$. The silicon thickness of 0.3 μm, nitride insulator thickness of 0.3 μm, source-drain voltage V_{sd} of 5 V are used.

Figure 2(b) shows the relation between the surface activation energy $E_S=E_c(0)-E_F$ and E_a^* which are calculated with the model gap density of states of Fig. 2(a) as previously explained. For higher temperatures the surface band bending is reduced as shown in Fig. 2(b) to conserve the induced charge for given gate voltage. This statistical shift of band bending affects the measurement of the activation energy as you see in Fig. 2(b). Thus the temperature dependent band bending as well as the spatial distribution of potential attribute to the difference between the surface band bending and measured activation energy as you see in Fig. 2(b).

Figure 3 shows the effect of deep states on E_a^* where the interface states $D(E)=0$, and Fig. 4 is for the various constant interface density of states. Closed circles in Fig. 4(b) represent the experimental results of Mackenzie *et al.*[3] In their experiment, the thickness of gate insulator and the silicon film were typically 0.3 μm each. The midgap densities of states or the constant interface states have a great effect in the lower gate voltage, but have small effect in the region above the threshold. The increase of these midgap states and the interface states does not alter the shape of the E_a^* at above the threshold.

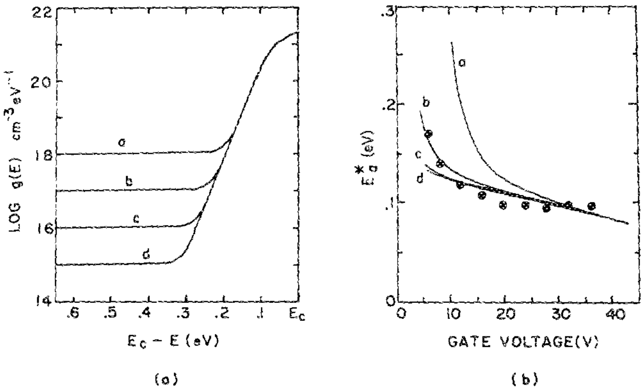

FIG. 3. The effect of deep gap states on E_a^*. The interface state is not considered, so that interface density of states $D(E)=0$. (a) is the model gap density of states and (b) is the calculated results of E_a^*. Closed circles represent the experimental results of Mackenzie *et al.* (see Ref. 3).

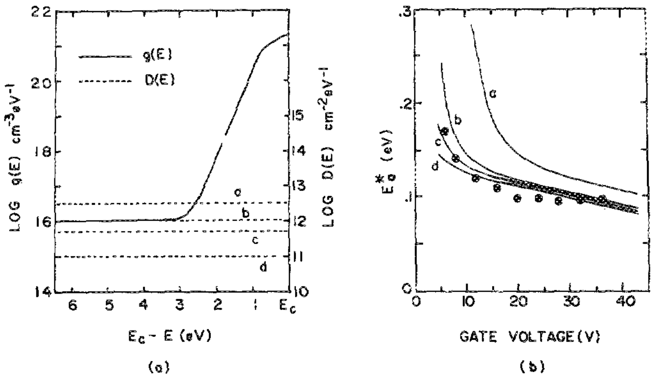

FIG. 4. The effect of different values of constant interface density of states on E_a^*. (a) shows the model gap density of states $g(E)$ (solid line) and the interface state densities $D(E)$ (dashed lines). (b) is the results of calculation for E_a^* using $g(E)$ and $D(E)$ of (a).

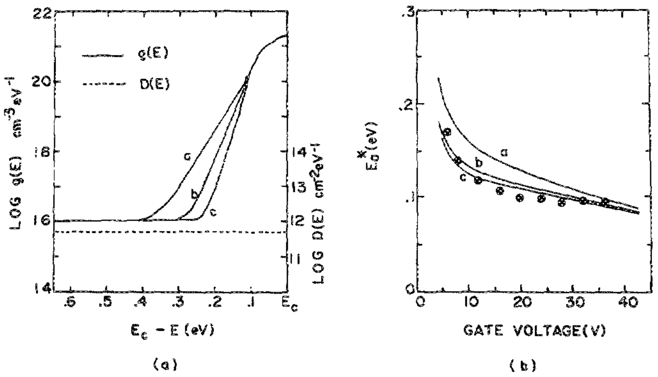

FIG. 6. The effect of change in characteristic temperature T_c of exponential tail on E_a^*. (a) depicts the $g(E)$'s with different tail widths a, b, and c and a constant $D(E)$. (b) shows the corresponding results for E_a^*. The fit with experiment at higher gate voltage is not satisfactory.

Figure 5 shows E_a^* for various width of exponential tail and constant interface density $D(E) = 5\times 10^{11}$ $\text{eV}^{-1}\,\text{cm}^{-2}$. The parallel shift of exponential tail by extending the width of linear region [Fig. 5(a)] give rise to a parallel shift of E_a^* as you see in Fig. 5(b). The E_a^* vs gate voltage curves are too steep to fit the experimental data [Fig. 5(b)].

The effect of the change in characteristic temperatures T_c of exponential tail on E_a^* is shown in Fig. 6. The increase of T_c has the effect of increasing the total gap densities and gives rise to a higher and steeper dependence of E_a^* on gate voltage. Thus the increase of T_c is not the answer. The measured E_a^* shows the typical features of slower decrease at higher gate voltage.

Comparing the results of our calculations with the experimental results, just the increase in deep states and in interface states do not give good fits to the results. The calculated curves so far gave steeper slope at higher gate voltage than experimental results no matter how the changes are made in the shape of band tails and the magnitude of gap and interface state density as long as they are constant.

Measuring the density of interface states of *a*-Si:H FET is difficult because it is not easy to separate the effect of gap states and that of interface states. The interface density of states measured by several methods are estimated to be 10^{11} to 10^{12} $\text{cm}^{-2}\,\text{eV}^{-1}$, but unfortunately this estimation was for the region near the Fermi energy. Thus the interface density of states for a higher level is not known for amorphous silicon yet.

In the case of crystalline MOSFET it has been known that the interface states had the *U* shape and increases as the energy level approaches the conduction band. In the case of hydrogenated amorphous silicon nitride it has been shown that the level of silicon dangling bond exists more or less near the conduction band edge of bulk *a*-Si:H.[7] Therefore we propose that the interface density near the conduction band edge is much larger, and we calculated the E_a^* for various distribution of interface states.

At first, E_a^* for steplike densities of states as shown in Fig. 7 (a) are used for calculation to obtain the E_a^* versus gate voltage curves as shown in Fig. 7(b). The width of larger interface density of states near conduction band is

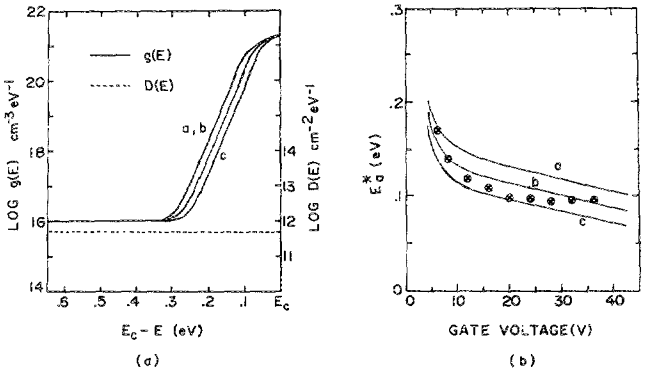

FIG. 5. E_a^* for parallel shift of exponential tail and a constant interface density $D(E) = 5\times 10^{11}$ $\text{cm}^{-2}\,\text{eV}^{-1}$. (a) shows the $g(E)$'s with shifted band tails a, b, and c together with a constant interface density. (b) shows the E_a^* vs gate voltage curves a, b, and c corresponding to $g(E)$'s a, b, and c.

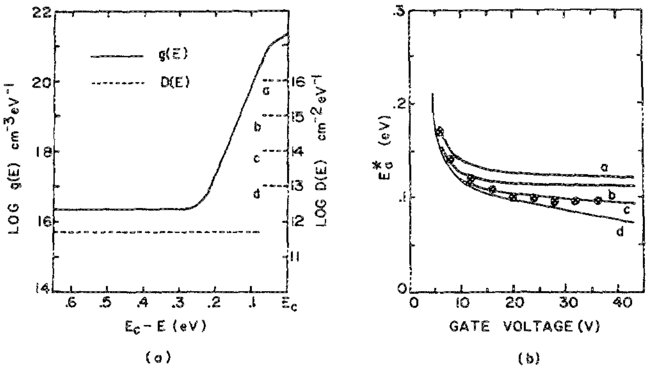

FIG. 7. The calculated field effect activation energy E_a^* for steplike interface densities of states. (a) The width of larger interface density of states near the conduction band edge is taken as 0.07 eV. (b) One can see much better fit even at higher gate voltage.

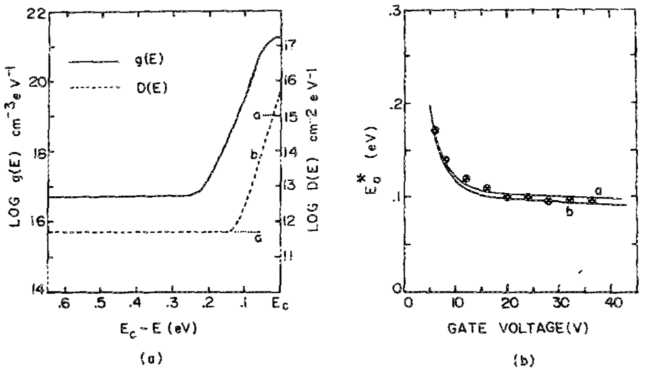

FIG. 8. The effect of interface states having exponential tail on E_a^*. (a) shows a $g(E)$ and $D(E)$'s with a flat top at 10^{15} cm^{-2} eV^{-1}, *a*, and an exponential tail all the way up to conduction band edge E_c. (b) shows the corresponding results for E_a^*, both of which have good fits with the experimental data.

taken as 0.07 eV. Comparing the experimental results, we see that this simple change gives the fairly good fit of E_a^* curves.

To see the effect of the distribution of interface states, we calculated the activation energy with the exponential interface states near the conduction band edge instead of flat interface state as shown in Fig. 8 (a) and the results are shown in the Fig. 8(b). Only small discrepancies with experiment are observed. Even though it is difficult to guess the exact shape of the distribution of interface states which fits best, it is certain that the density of interface state near the conduction band edge must be much larger.

IV. CONCLUSION

The field effect activation energy E_a^* was investigated. The E_a^* was calculated for various model gap and interface state densities. From the comparison of the experimental results and the numerical calculation we propose that the density of interface states is much larger near the conduction band edge.

[1] N. Lustig, J. Kanicki, R. Wisnieff, and J. Griffith, MRS Symp. Proc. **118**, 267 (1988).
[2] N. Lustig and J. Kanicki, J. Appl. Phys. **65**, 3951 (1989).
[3] K. D. Mackenzie, A. J. Snell, I. French, P. G. LeComber, and W. E. Spear, Appl. Phys. A **31**, 87 (1983).
[4] F. Djamdji and P. G. LeComber, Philos. Mag. B **56**, 31 (1987).
[5] M. Shur, C. Hyun, and M. Hack, J. Appl. Phys. **59**, 2488 (1986).
[6] M. Shur and M. Hack, J. Appl. Phys. **55**, 3831 (1984).
[7] J. Robertson and M. J. Powell, MRS Symp. Proc. **49**, 215 (1985).